PERGAMON

International Journal of Heat and Mass Transfer 45 (2002) 4315–4324

International Journal of HEAT and MASS TRANSFER

www.elsevier.com/locate/ijhmt

Effects of preheating and operation conditions on combustion in a porous medium

Y. Huang, C.Y.H. Chao *, P. Cheng

Department of Mechanical Engineering, Hong Kong University of Science and Technology, Clear Water Bay, Kowloon, Hong Kong

Received 18 February 2001; received in revised form 18 March 2002

Abstract

The effects of preheating conditions (including the critical energy content, the firing rate, and the equivalence ratio) on the initiation and extinction of a super-adiabatic combustion (SAC) in a steady flow of propane/air mixture through a stack of stainless steel screens (an inert porous medium) are investigated. It is found that there are critical conditions for the initiation and extinction of a SAC in the steady flow through the inert porous column. The critical preheating energy required to initiate a SAC is found to decrease with the increase of the preheating equivalence ratio, the preheating firing rate, and the operational equivalence ratio. After the initiation of a SAC, two combustion modes (i.e., stable combustion mode and push-forward combustion mode) have been observed. These combustion modes are determined by the operational conditions.

1. Introduction

Environmental protection and energy saving are two important issues for maintaining a sustainable environment. These two issues happen to have a close relationship in the field of combustion, especially for combustion in a porous medium. For environmental protection point of view, the pollutant emissions including CO, UHC, and NO_x, etc. from a combustor or furnace, should be reduced as much as possible. Unfortunately, it is rather difficult to get rid of all of these pollutants simultaneously, because the contradictory trends of their concentration change with respect to temperature. It is known that the best way to minimize pollutant emissions from a combustor or furnace is to limit the temperature of combustion in a narrow band [1], say 1670–1900 K, for the purpose of keeping the concentrations of all of these pollutants to be very low. The corresponding combustion techniques include rich flame-quick mixing (RQ) [2], lean premixing (LP) [3] and etc.

The development of porous combustors provides an excellent choice to solve the problem of pollution emission. It is known that combustion in porous media can greatly broaden the weak limit, increase the maximum temperature (for the burning of toxic gases) and flame propagation speed, and enhance the stability of flames and the ability to burn the fuel/air mixture with very low-heat value. This is because the inner heat recirculation process (due to the porosity of the medium) enables the incoming fuel–air mixture to absorb radiant heat from the hot exhaust gas in the downstream, without direct contact between them. This implies that it is possible to initiate combustion at a temperature below the narrow band that was mentioned above, and keep the concentrations of all the pollutants to be very low. Furthermore, this means that many exhausted toxic gases could be burned as a new energy resource for industrial uses, thus reducing the environment pollution and saving energy simultaneously.

In recent years, the study of combustion in porous media has attracted a great deal of attention. Both Viskanta [4] as well as Kaviany and Oliveira [5] have reviewed recent development on this topic. Viskanta [4] focused his attention on combustion of porous radiation burners (PRB) made of a porous inert medium (PIM), while Kaviany and Oliveira [5] paid more attention to the thermophysical and thermochemical nonequilibria processes within different phases. Many new concepts have

* Corresponding author. Tel.: +852-2358-7210; fax: +852-2358-1543.

E-mail address: meyhchao@ust.hk (C.Y.H. Chao).

0017-9310/02/$ - see front matter
PII: S0017-9310(02)00137-0

been proposed. Among them are resonance between a thermal wave and a combustion wave [6], bi-stable combustion in two different domains [7], double wave phenomena with cellular structure [8], low-temperature wave [9] or super-adiabatic combustion (SAC) [10,11] in a PIM, and heat recirculation [12]. These new concepts have opened new avenues for investigation of combustion phenomena in PIM. Thus, the stability limits, maximum combustion temperature, and heat recirculation by radiation were investigated by many researchers both experimentally and numerically.

The first scientific demonstration of super-adiabatic temperatures was given by Egerton et al. [13] about 30 years ago when they examined the mechanism of smoldering in cigarettes. Echigo [11] reported that a drastic decrease in enthalpy of an outflowing gas (at more than 300 K) can be achieved with the addition of a porous plug made of a form metal with a thickness in the order of 10^{-2} m. Based on these findings, he then proposed a new concept for furnace design that would save energy. Sathe et al. [14] investigated the radiation efficiency of a porous radiant burner under steady flow conditions using methane as a fuel with equivalence ratio of 0.55–0.6. They found the flame width to be about 2.5 mm with the flame speed about 120 mm/s. By a proper control of firing velocity, the flame could be stable at two locations: in the upstream half and the downstream edge of the porous medium. The radiation efficiency that they measured was about 26–40% when the buried flame was in the upstream half of the porous medium. Min and Shin [15] observed the existence of low temperature and low-burning velocity flame in a steady flow of propane using honeycomb ceramic as PIM. They suggested a dimensionless mass-flow-rate-ratio instead of the absolute firing rate to be one of the parameters that affect the performance of combustion in PIM. Kennedy et al. [8] studied the flame structures and their instabilities from both steady flow and oscillating flow combustion in PIM using methane, hydrogen, and acetylene as fuels. They attributed the formation of the flame structure to a thermodiffusive instability of pore-level-driven combustion [16]. Zhdanok et al. [6] reported some resonance condition between a thermal wave and a combustion wave with a propagating speed of about 0.2 millimeter per second when the equivalence ratio was about 0.259 using methane as fuel and solid spheres as the porous medium. They found that the maximum temperature in this wave was approximately 2.8 times the normal adiabatic temperature. Their reports suggested the existence of two modes, i.e., a push-forward flame mode and a flame extinguished (or pure thermal wave) mode. Mital et al. [17] studied some porous ceramic radiant burners using methane as a fuel. They used three different diameters of thermocouple beads to estimate the actual high temperature by extrapolating the data to zero bead diameter thermocouple. They found that the lift-off limit was between equivalence ratio of 0.6–0.7, and the lean limit was between 0.5 and 0.6 for the PRB with a firing rate of 150–650 kW/m^2. They reported that radiation efficiency was between 20% and 31%, while the flame speed was rather slow between 50 and 150 mm/s for the range of 157–473 kW/m^2 at an equivalence ratio of 0.9, comparing with the adiabatic flame speed of 350 mm/s for methane. Bouma and De Goey [18] investigated both experimentally and numerically the emission of NO_x from ceramic foam burners, and confirmed the existence of stable combustion mode, i.e., the flame was fixed at a location buried in a PIM.

In a recent paper, Zhdanok et al. [6] suggested that the temperature of the reaction zone was affected by the initial heating condition, which was used as a parameter for the control of the reaction rate. It appears that the effect of preheating is a unique character of combustion in porous medium although not much work has been devoted to the study of this effect. It can be speculated that different initial preheating conditions and different operation conditions may affect the initiation and extinction of a flame as well as the subsequent combustion modes in a porous medium. This paper attempts to study some aspects of these problems.

2. Experimental setup

Fig. 1 shows the experimental setup, which consisted of a gas and fuel supply system, an insulated porous medium combustor, and a measuring and data

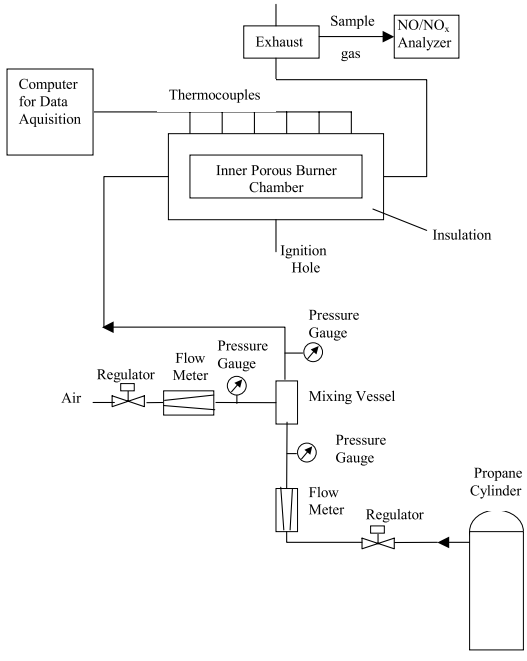

Fig. 1. Experiment setup.

acquisition system. To initiate a SAC in a PIM, a high enough energy content should be placed into the PIM. In practice, the most common way to start a SAC in a PIM is to use a hot jet with a high equivalent ratio to establish a flame so that a small part of PIM is preheated. Such a method was used to initiate a SAC in PIM in the present experiment.

2.1. Gas and fuel supply system

Propane was used as the fuel in this experiment because of its availability. The propane released from a container and the compressed air were regulated and metered separately before entering a mixing vessel. The mixing vessel was used to make the fuel–air mixture more uniform spatially and maintain the equivalence ratio of mixture (which is proportional to the fuel/air mixture) at the same level during the experiment time duration. Three pressure gauges were installed downstream of the flowmeters for air, fuel, and mixture. These pressures were measured in order to calculate the compensated volume flow rates of air and fuel and the flow velocity of the mixture. After passing through the mixing vessel, the air–fuel mixture entered the porous medium burner. The products of combustion were let out through the exhaust pipe.

2.2. Combustor

The combustor was made of an inner burner chamber (which also served as the porous media holder), insulation, and an outer rectangular box. The inner burner chamber was made of a stainless steel cylinder with a length of 480 and 105 mm in diameter. Two diffuser sections connected to each end of the cylinder to the inlet and outlet gas pipes. The variable cross-sectional areas of the diffuser sections (see Fig. 2) help to confine the free standing flame inside the combustor under a wider range of equivalence ratios. The outer rectangular box was made of 1.5 mm thick stainless steel plate. The cross-sectional area of the box was 210×210 mm^2. Between the chamber and the outer box, it was filled with kaowool for insulation. A hole was drilled through the mid-section of the box, the insulated material, and the burner chamber for pilot flame ignition.

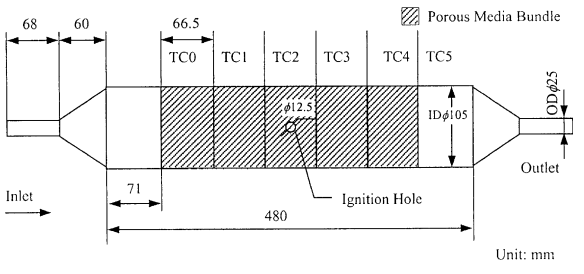

Fig. 2. Inner burner chamber.

2.3. Porous medium

In our experiments, five bundles of stainless steel wire screens (8 meshes per inch) were used as the porous medium. The length of each bundle was 66.5 mm. Pieces of stainless steel wire screen were first cut into a circular shape 4 inches in diameter. The five bundles of screens were stacked together to form a porous column of 332.5 mm in length and packed inside the cylindrical chamber.

2.4. Measuring and data acquisition system

Six thermocouples were inserted in the narrow space between the five bundles of wire screens for measurements of gas temperature (see Fig. 2). Since we intended to investigate low-equivalence ratio combustion with a maximum temperature below 1250 °C, the standard RS 219-444 thermocouples were used, which had a 0.5 mm diameter sheath and 2 s response time. These thermocouples were connected to a PC through a data acquisition system, which included a SCXI-1303 terminal block as connection kit and cold junction compensation, a SCXI-1102B multiplex amplifier as signal conditioning module, a SCXI-1000 slot chasis, and a PCI-6023E MIO board as A/D converter. LabView software was used in the data acquisition program.

3. Experimental procedure

As mentioned earlier, the primary aim of the present paper is to study the effect of preheating on the initiation of a SAC in the PIM, and the effects of the operation condition on its subsequent combustion phenomena. The experimental procedure was divided into two stages. The first stage was to set up a stable free stream flame located between the inlet diffuser and the leading edge of the PIM (shown as Fig. 2). Therefore, three different initial parameters (such as fuel flow rate, air flow rate, and the time duration), resulted in different preheating conditions that affect the initiation of a SAC. Because of the difficulty to ignite the fuel–air mixture in a wide range of initial parameters, the first stage of the procedure was divided into two steps: the first was the ignition step (approximately 1 s in duration) during which a rather fuel-rich mixture was supplied to the combustor for ignition; and the second was the preheating step in which the parameters were switched immediately to the expected preheating condition once the mixture was ignited. The second stage was to switch the parameters to the operation condition with a smaller fuel/air mixture. The independent variables in the preheating stage are the fuel flow rate, air flow rate, and the time duration

while the independent variables in the operating stage are the fuel flow rate and the air flow rate.

4. Experimental results and discussion

Because combustion in a PIM depends on geometric and material factors such as size, shape, capacity etc., it is more appropriate to use the following three dimensionless parameters for the presentation of experimental results:

(1) The dimensionless preheating energy content e_i in the PIM is defined as:

$$e_i = \frac{\Delta E}{m_s C_{Ps} \Delta T_0} \tag{1}$$

where m_s denotes the mass of solid matrix of the PIM ($m_s = 1950$ g in the present experiment), C_{Ps} denotes the specific heat capacity of the solid matrix, ΔT_0 denotes a reference temperature rise ($\Delta T_0 = 1000$ K was chosen), and ΔE denotes the energy input into the PIM which can be calculated from $\Delta E = \dot{m}_f q_f \Delta t$ with $\dot{m}_f$ being the mass flow rate of fuel, q_f being the calorific value of fuel, and Δt being the time duration of preheating.

(2) For the firing rate, a dimensionless mass-flow-rate ratio r, similar to those suggested by Min and Shin [15], is used in the present paper as follows:

$$r = \frac{\dot{m}_m}{\rho_f U_0 A} \tag{2}$$

where $\dot{m}_m = \dot{m}_f + \dot{m}_a$ is the mass flow rate of the fuel/air mixture (with $\dot{m}_a$ denoting the mass rate of air), ρ_f is the density of fuel, U_0 is the maximum laminar flame propagation velocity of the fuel (at atmospheric pressure and room temperature), which is 464 mm/s for propane [19], and A is the flow passage cross-sectional area which was 61.46 cm^2 in the present apparatus with the PIM in combustor.

(3) The equivalence ratio is defined as

$$\Phi = \frac{\left(\dot{m}_f/\dot{m}_o\right)_{\text{actual condition}}}{\left(\dot{m}_f/\dot{m}_o\right)_{\text{stoichiometric condition}}} \tag{3}$$

where $\dot{m}_o$ is the mass flow rate of the oxidiser. Eq. (3) is a ratio comparing the actual fuel and oxidiser ratio to the stoichiometric fuel to oxidiser ratio when complete conversion of the fuel to carbon dioxide and water is assumed. An equivalence ratio higher than 1 indicates a fuel-rich condition while an equivalence ratio lower than 1 means that the condition is fuel lean.

The three independent dimensionless parameters during the preheating stage are the energy content e_i, the equivalent ratio Φ_i, and the dimensionless firing rate r_i. Note that the energy content in the preheating stage has taken into consideration the preheating time Δt while the equivalence ratio and the firing rate can influence the temperature distribution across the porous medium. On the other hand, the two independent dimensionless parameters in the operation condition are the equivalent ratio Φ_{op} and the dimensionless firing rate r_{op}. In the following paragraphs, the effects of the preheating condition to start a SAC, and the effects of operation condition on combustion modes in a PIM will be discussed.

4.1. Effects of preheating energy content

As mentioned earlier, it is unnecessary to preheat uniformly along the PIM to initiate a SAC. The preheating energy content in the PIM was added only on upstream part of PIM as had been done by all previous researchers. In the present experiments, the energy during preheating was added mostly on the first bundle of the screens because the flame was usually stabilized in the diffuser ahead of the PIM.

Fig. 3a shows the temperature variation at different locations during the first 200 s at the preheating condition of $e_i = 0.75$, $\Phi_i = 1.0$, $r_i = 0.18$. The corresponding temperature distribution along the PIM at $t = 200$ s is

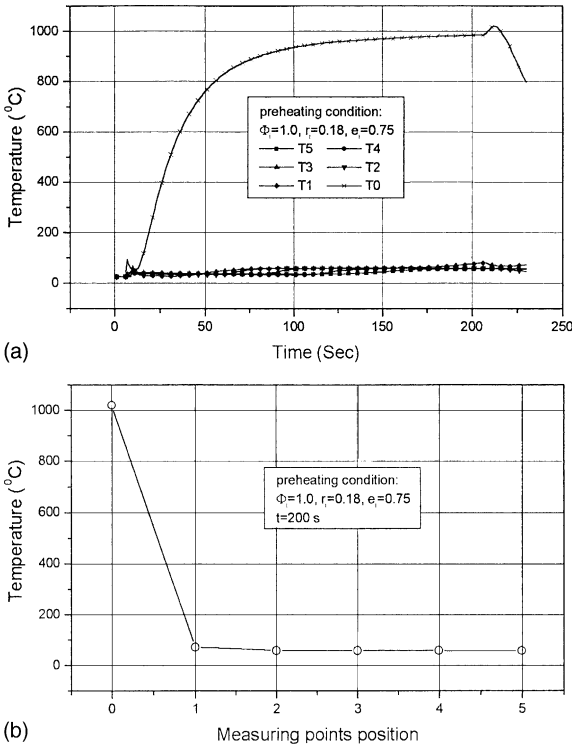

Fig. 3. (a) Temporal temperature variations during preheating and (b) temperature profile along PIM during preheating.

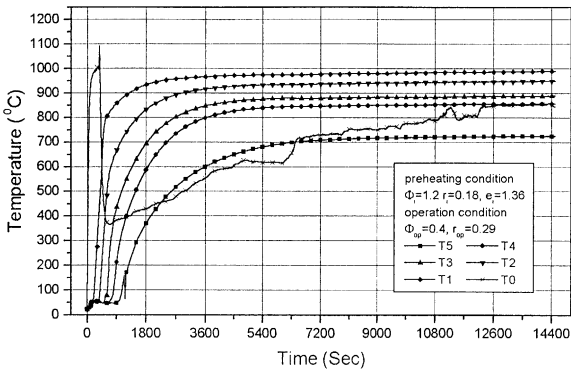

Fig. 4. Temporal temperature variations in a stable combustion mode.

shown in Fig. 3b. It is seen from Fig. 3a and b that the temperature at the position 0, which is denoted as T_0 and located at the upstream edge of the PIM, had risen to about 1000 °C just before switching to the operation condition at $t = 200$ s, while the temperatures of other positions remained unchanged. The results imply that energy was added only on the upstream part of the PIM, about 20% of the total PIM from T_0 to T_1.

Figs. 4 and 5 show the effect of operational equivalence ratio ($\Phi_{op} = 0.4$ or $\Phi_{op} = 0.28$) on the combustion mode when the preheating energy content is sufficiently large ($e_i = 1.36$ for example), and at an initial firing rate of $r_i = 0.29$ and the initial equivalence ratio of $\Phi_i = 0.4$. Note that the maximum temperatures in Figs. 4 and 5 were close to 1000 and 900 °C, respectively, which are greater than the adiabatic flame temperatures, estimated to be about 870 and 450 °C [8], respectively, under the corresponding equivalence ratio. Thus, it can be concluded that a SAC had been initiated in Figs. 4 and 5. Fig. 4 with $\Phi_{op} = 0.4$ shows that, with the exception of T_0, all other temperatures reach to different constant values as time increases which are the characteristics of the stable combustion mode. The maximum temperature was given by T_1 (corresponding to TC1 in Fig. 2) located in the upstream half of PIM. This suggested that a flame occurred between TC0 and TC1. The temperature variation of T_0 was most interesting. After switching to the operation condition, the fuel–air mixture was no longer flammable in the empty diffuser section. Since no free stream combustion occurred in the space upstream of the PIM, so, T_0 decreased immediately after switching to the operation condition. With the help of stored heat energy in the PIM, a SAC was subsequently set up at a location upstream of TC1, resulting in an increase of T_0 gradually, although with rather large fluctuations due to the dynamic influence of incoming cold flow and the heat recirculation from downstream parts by radiation.

Fig. 5 shows the temporal temperature variations when the operating equivalence ratio is $\Phi_{op} = 0.28$ with the other parameters the same as in Fig. 4. It is shown that at a smaller operational equivalence ratio, the temperature at each position first increased, maintaining a constant value, and then suddenly decreased. The sudden drop in temperature indicated the flame had passed through that location during that instant of time. We therefore can identify this temperature variation as a push-forward combustion mode of a SAC. This combustion mode was also observed by Zhdanok et al. [6], who presented their data for temperature variations with axial distance at specific times. A comparison of Figs. 4 and 5 shows that a stable combustion flame can not be maintained with a small operational equivalence ratio. This is because a decrease of operation equivalence ratio would result in less heat recirculation to the incoming fuel–air mixture, and therefore, there was insufficient heat to sustain a stable combustion at a fixed position. It can be concluded from Figs. 4 and 5 that the operation equivalence ratio determines the combustion mode after a SAC has been initiated.

Fig. 6 shows temperature variations for the case where Φ_i, r_i, Φ_{op}, r_{op} have the same values as those of Fig. 4 but with different initial energy content ($e_i = 1.36$

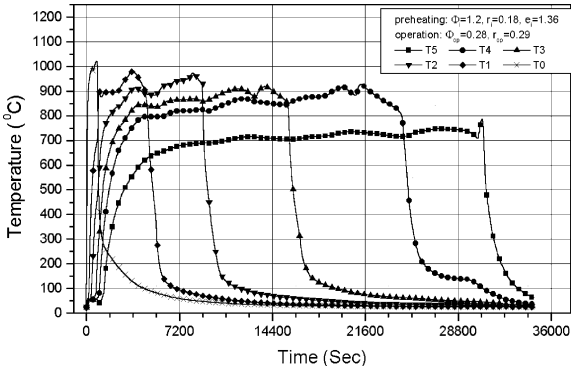

Fig. 5. Temporal temperature variations in a push-forward combustion mode.

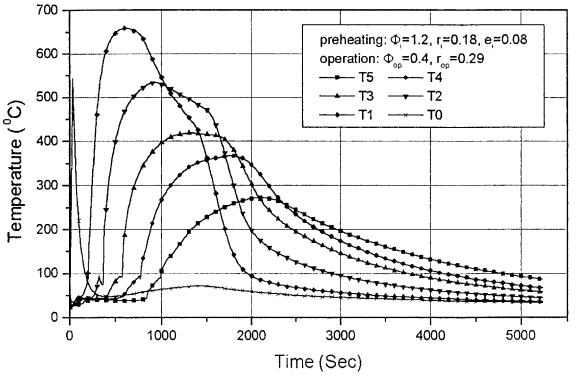

Fig. 6. Temporal temperature variations in a flame extinction mode.

in Fig. 4 and $e_i = 0.08$ in Fig. 6). It is seen from Fig. 6 that the temperature first increased and then decreased with time. With a small preheating energy content of $e_i = 0.08$, the maximum temperature did not exceed 650 °C indicating that no SAC had been initiated. Therefore, this case was a pure thermal wave without a flame. It can also be concluded that a SAC could not be initiated due to insufficient preheating energy content. Thus, although the flame location and the combustion mode (stable or push-forward) is influenced by the operation equivalence ratio as discussed in Figs. 4 and 5, the initiation of a SAC is influenced mainly by the amount of preheating energy content e_i as shown in Figs. 4 and 6.

It should be noted that part of the energy from the combustion during the preheating stage was lost through the exhaust gas stream and part of the heat content was stored in the burner shell. The exhaust gas temperature was approximately 50 °C. Under a typical preheating time of 60 s and a typical total mixture flow rate of around 0.0019 kg/s, a comparison to the total energy content (about 350 kJ) indicated that heat loss to the exhaust stream was about 1% of the total energy content. It was, however, difficult to quantify how much energy was used to heat up the burner shell but this amount did not vary too much from one case to another as the average temperature across the burner did not deviate too much from each other, as shown in Figs. 4 and 5 (in the order of magnitude around 800–900 °C when a SAC was initiated in our experimental conditions). A TESTO M300 gas analyser was also used to monitor the CO/O_2 concentrations in the exhaust gas, and the combustion efficiencies were around 99% in all the cases during preheating stage.

4.2. Effects of preheating firing rate

We now investigate the effect of preheating firing rate r_i (at a specific preheating equivalence ratio $\Phi_i = 0.95$) on the initiation of a SAC during a specific operation condition of $\Phi_{op} = 0.4$ and $r_{op} = 0.23$. The results of this investigation are presented in Fig. 7, which is a plot of the critical preheating energy content e_{cr} versus the preheating firing rate r_i. The procedure of obtaining the value of e_{cr} in Fig. 7 is described below. Consider a specific preheating firing rate of $r_i = 0.14$ and the procedure of obtaining the value of e_{cr} corresponding to this firing rate consisted of the following two steps. As will be discussed in connection of Fig. 9, $\Phi_{op} = 0.4$ with $\Phi_i = 0.95$ and a large value of e_i (i.e., a relatively large value of Δt) will ensure a stable combustion mode once the mixture is ignited. Thus, the first step was to choose a relatively large value of preheating duration Δt to ensure that a SAC could be initiated. Then, the mixture in the porous column was ignited and the preheating condition of $\Phi_i = 0.95$ and $r_i = 0.14$ and a relatively large value of Δt was imposed. Subsequently, the operation condition of $\Phi_{op} = 0.4$ and $r_{op} = 0.23$ was switched on to see whether the stable combustion mode was sustainable. The second step began after the porous column was cooled down. During the second step, the mixture was first ignited and the preheating condition of $\Phi_i = 0.95$ and $r_i = 0.14$, and a very small value of e_i was then imposed. A small value of Δt was chosen to ensure the existence of the no flame condition in the porous column. The same operation condition of $\Phi_{op} = 0.4$ and $r_{op} = 0.23$ was then switched on to see whether no flame condition would remain. The above two steps were repeated sequentially with smaller Δt in the first step and a larger Δt in the second step until the critical preheating energy content e_{cr} was identified. Thus, the value of e_{cr} can be considered to be the critical preheating energy content to sustain a stable combustion mode when viewing from the top along the vertical axis (at $r_i = 0.14$) in Fig. 7. It may also be considered as the critical preheating energy for the initiation of a SAC when viewing from the bottom along the vertical axis of $r_i = 0.14$ from the no flame region to the stable combustion region.

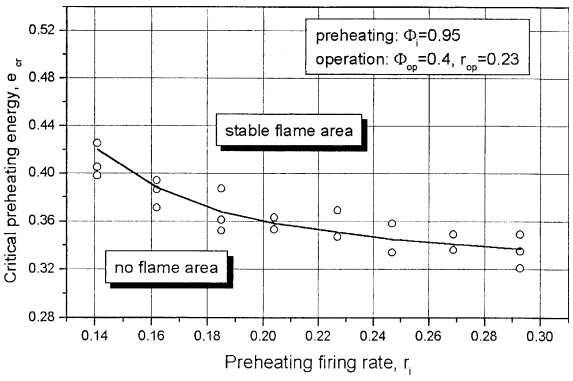

Fig. 7. Critical preheating energy content versus preheating firing rate.

The experimental data shown in Fig. 7 were obtained for eight different preheating firing rates. Note that at each preheating firing rate, two or three experimental runs were repeated to check its repeatability. A solid curve was drawn through the data points dividing into an upper stable flame region and the lower no flame region. The no flame region can also be interpreted from the increasing or decreasing preheating firing rates point of view as follows. To be specific, consider the horizontal line of $e_i = e_{cr} = 0.36$ that crosses the solid curve at $r_i = 0.20$. If the preheating firing rate r_i is increased from zero, the initiation of a SAC would occur as the firing rate is increased to $r_i = 0.20$. Under this situation, $r_i = 0.2$ is the critical preheating firing for the initiation of a SAC. Next, consider the decrease of the firing rate in the stable combustion mode along the horizontal line of $e_i = e_{cr} = 0.36$. The stable combustion mode can no longer be sustainable as the preheating firing rate de-

creases to the value of $r_i = 0.20$. Thus, this value can be interpreted as the critical preheating firing rate for which stable combustion is sustainable.

We now consider the trend in Fig. 7 from the decrease of preheating firing rate point of view. The decrease of preheating firing rate would lead to three results, namely: (1) the preheating energy will be confined within a narrower region of the PIM, which makes a more effective preheating for the initiation of a SAC, (2) the heat transfer from hot jet to solid matrix would decrease, thus will increase the temperature difference between solid and gas, and (3) most importantly, the flame location during preheating in the diffuser will move further upstream, thus affecting the effectiveness of preheating dramatically. Fig. 7 shows that the critical preheating energy required to initiate a SAC increases with the decreases of firing rate. This means the effects of (2) and (3), which result in greater temperature difference between the hot gas and the solid matrix, are stronger than that of (1), especially at small firing rates. Note that the solid curve in Fig. 7 approaches a horizontal line of $e_{cr} = 0.34$ at large r_i, which implies that it is impossible to initiate a SAC if $e_i < 0.34$ under the preheating condition of $\Phi_i = 0.95$, and the operational condition of $\Phi_{op} = 0.4$, and $r_{op} = 0.23$.

4.3. Effects of preheating equivalence ratio

Next, we study the effect of preheating equivalence ratio Φ_i (with a preheating firing rate of $r_i = 0.23$) on the initiation of a SAC during a specific operation condition of $\Phi_{op} = 0.4$ and $r_{op} = 0.31$. The results of this study are presented in Fig. 8 where the critical preheating energy content e_{cr} versus the preheating equivalence ratio Φ_i is plotted. As will be discussed in connection with Fig. 9, the operation condition determine the combustion modes, and the value of $\Phi_{op} = 0.4$ indicates that a stable combustion mode exists if a SAC has been initiated. Thus, the value of e_{cr} can either be considered as the critical preheating energy for an initiation of a SAC or as the critical preheating energy for the extinction of a stable combustion. It can be seen from Fig. 8 that the critical preheating energy e_{cr} decreases dramatically with the increase of the preheating equivalence ratio Φ_i when $\Phi_i < 0.7$. The reason for this behavior can be explained as follows. As the preheating equivalence ratio is increased, the maximum gas temperature during preheating should increase, resulting in better heat transfer between hot gas and solid matrix and more heat storage in the PIM. Thus, the increase of the preheating equivalence ratio would decrease the critical energy required to initiate a SAC. From another point of view, the decrease of the preheating equivalence ratio would increase the critical preheating energy to sustain a stable combustion mode in the porous column. It is interesting to note that the preheating equivalence ratio has no effect on the critical preheating energy content when $\Phi_i > 0.7$. Also, it is interest to note from Fig. 8 that it is impossible to initiate a SAC if $e_i < 0.34$ under the condition of $r_i = 0.23$, $\Phi_{op} = 0.4$, $r_{op} = 0.31$.

4.4. Effects of operational equivalence ratio

Fig. 9 is a plot of the experimental data of critical preheating energy e_{cr} versus the operation equivalence ratio Φ_{op} at the preheating conditions of $\Phi_i = 1.2$ and $r_i = 0.18$, and the operation firing rate of $r_{op} = 0.29$. The data point for equivalence ratio of 0.57 (i.e., the lean flammability limit of the propane/air mixture) was extracted from Ref. [19] from combustion without a porous medium, which was not obtained from our experiment. With an increase of the operational equivalence ratio Φ_{op}, the fuel/air mixture becomes more flammable, and therefore, the critical preheating energy required to start a SAC should decrease.

Fig. 9 shows that regions of stable and push-forward combustion, and dissipating thermal waves (no flame) exist for different values of the preheating energy e_i and

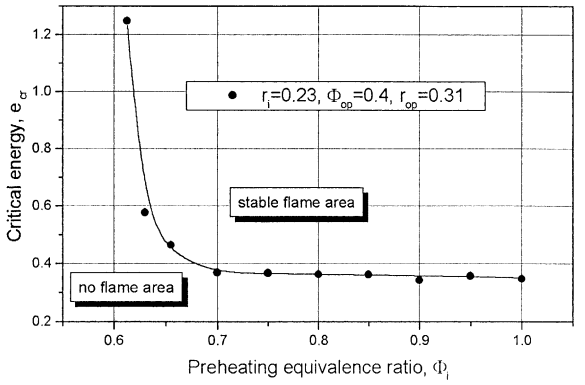

Fig. 8. Critical preheating energy content versus preheating equivalence ratio.

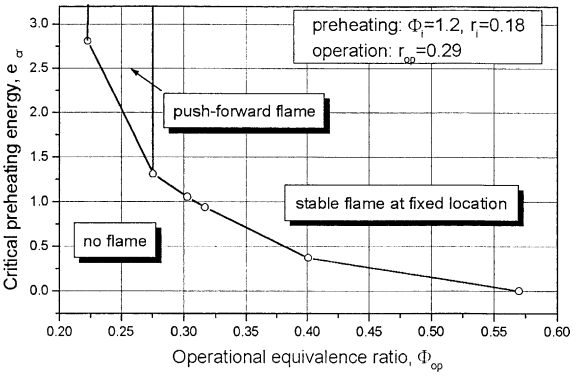

Fig. 9. Critical preheating energy content versus operational equivalence ratio.

the operating equivalent ratio Φ_{op}. If the operational equivalence ratio $\Phi_{op} < 0.22$, no flame can occur. When $0.22 < \Phi_{op} < 0.28$, the increase of the preheating energy will switch the temperature pattern from no flame to push-forward combustion. When $\Phi_{op} > 0.28$, an increase of initial preheating energy will switch the temperature pattern from no flame to stable combustion. It was found between each of these patterns, there were some sensitive bands in which what combustion mode could occur is uncertain. Fig. 9 shows that the initiation of a SAC is possible even if the operational equivalence ratio is less than the lean flammability limit of the propane/air mixture (i.e., $\Phi_{op} = 0.57$) if some amount of preheating is carried out.

4.5. A low-temperature reaction zone

Fig. 10 shows the temporal temperature variations for the case of the preheating condition of $e_i = 0.14$, $\Phi_i = 1.0$, $r_i = 0.14$ and the operation condition of $\Phi_{op} = 0.4$, and $r_{op} = 0.29$. According to Fig. 9, no flame can exist in the porous column under such conditions. We noticed, however, that T_1 in Fig. 10 decreases rather slowly between the time period from $t = 400$ to 1200 s (corresponding to the temperature range between 600 and 300 °C), which seems to be distinctly different from that of a pure thermal wave reported earlier by Zhdanok et al. [6]. Similar temperature variations also exist in Fig. 6.

To investigate this phenomenon further, we conducted another experiment with an increase of the preheating energy content from $e_i = 0.14$ to 0.39 and with all other parameters remained the same as in Fig. 10 (i.e., $\Phi_i = 1.0$, $r_i = 0.14$, $\Phi_{op} = 0.4$, and $r_{op} = 0.29$). Note that the value of $e_i = 0.39$ is near the critical preheating energy for the initiation of a SAC. The temporal temperature variations for this case are presented in Fig. 11, which is slightly different from those in Fig. 4 for the stable combustion mode with a large value of e_i ($e_i = 1.36$). Fig. 11 shows that the temperatures T_1 and T_2 experienced a multi-step variation. They increased initially from $t = 0$ to 600 s because of the heat transfer by pure thermal wave from upstream PIM. Then, these temperatures decreased slightly from $t = 600$ to 1300 s because no SAC was immediately started. From $t =$ 1300 to 4100 s, T_1 and T_2 were at constant temperatures of 750 and 600 °C respectively, which we shall refer to as a "low-temperature reaction zone". Subsequently, the temperature rosed abruptly because of the initiation of a SAC resulting in a temperature of about 980 °C, which has been called a low-temperature combustion mode by Koester et al. [9]. However, the mechanism for the nearly constant temperature at 750 °C during the period from $t = 1300$ to 4100 s is not clear. Obviously, it could not be called an extinguishing flame because the temperature did not go down as a pure thermal wave. And, of course, it could not be called a SAC either because the temperatures were obviously smaller than 980 °C. A possible explanation for this phenomenon is that there must be some additional heat input into the PIM, thus resulting in the slower rate of temperature decrease from $t = 1300$ to 4100 s. We speculate that this additional energy is owing to a super-low-temperature reaction because of the partial conversion of the chemical energy in fuel to heat. In order to verify the above speculation, a direct contrast experiment was conducted and the results are shown in Fig. 12. In the contrast experiment, all the parameters were kept the same as those in Fig. 10, except that the fuel was cut off at the moment $t = 500$ s. A comparison of Figs. 10 and 12 shows that the agreement of data before $t = 500$ s is satisfactory. After the cut off time, the temperature T_1 in Fig. 12 dropped off much faster than that in Fig. 10. Since T_1 in Fig. 10 is higher than in Fig. 12 (with fuel shut off at $t = 500$ s) during the period of $t = 600$–1600 s, it suggested that low-temperature reactions had

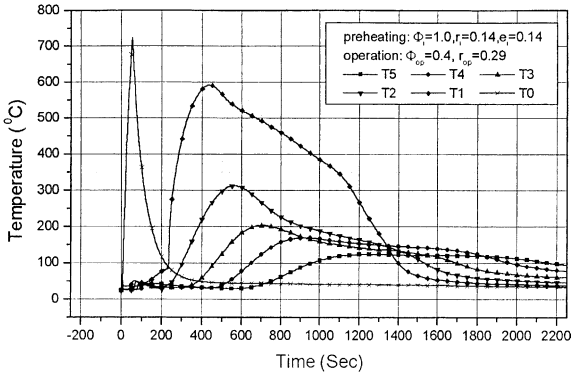

Fig. 10. Temporal temperature variations in a flame extinction mode.

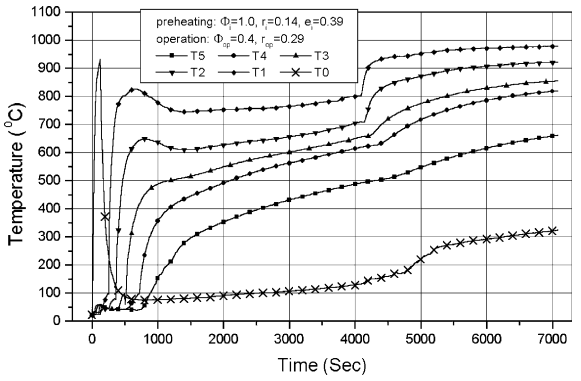

Fig. 11. Temporal temperature variations in a stable combustion mode with critical preheating energy content.

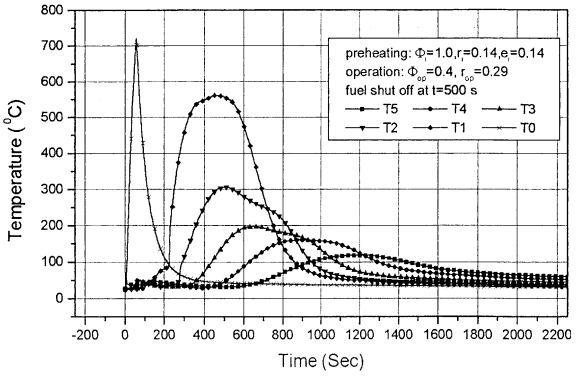

Fig. 12. Test similar to Fig. 9 with fuel shut-off at $t = 500$ s.

occurred between T_1 and T_2 during that period of time in Fig. 10. This low-temperature reaction phenomenon in the present experiment may be interpreted from the view point of alkane chemistry discussed by Pilling et al. [20], who stated that propane and larger alkanes have low-temperature chemical reactions at a temperature between about 500 and 1000 K.

5. Conclusions

Several conclusions can be drown from the present experiments as follows:

1. The preheating of the PIM has great influence on the initiation and extinction of a SAC during operation condition. The critical preheating energy content for the initiation and extinction of the SAC depends on the firing rate and the equivalence ratio during both the preheating and the operation stages. The critical preheating energy required to start a SAC decreases as the operational equivalence ratio is increased to the lean flammability limit of the fuel.
2. The firing rate in preheating has only small influence on the critical preheating energy content for the initiation of a SAC. The value of this critical preheating energy content decreases slightly with the increase of preheating firing rate. On the other hand, the preheating equivalence ratio seems to have great influence on the critical preheating energy content when the preheating equivalence ratio is less than 0.7. In this range of preheating equivalence ratio, the critical preheating energy content decreases dramatically as the preheating equivalence ratio is increased. When the preheating equivalence ratio is greater than 0.7, it has no effects on the critical preheating energy content.
3. At least two combustion modes, i.e., the stable combustion mode and the push-forward combustion mode are confirmed in the present experiments.
4. After a SAC has been initiated, the combustion modes are determined by the operational conditions characterized by the equivalence ratio and the firing rate.
5. With the increase of operational equivalence ratio, the combustion mode shifts from the push-forward mode to stable combustion mode.
6. A low-temperature reaction zone ranging from 600 to 900 °C in the no flame region of the propane/air mixture in the PIM has been observed.

Acknowledgements

The authors would like to acknowledge the financial supports of this work by the Research Grant Council of Hong Kong through Project no. HKUST6016/98E and DAG 98/99.EG29. They would like to thank Mr. Z.P. Zeng for his assistance in the experiments.

References

[1] A.H. Lefebvre, Gas Turbine Combustion, second ed., Taylor & Francis, London, 1999.
[2] B. Simon et al., Possibilities and limitations of reducing pollution by aeroengines by modification of the combustion process, in: Proceedings of Future Civil Engines and the Protection of the Atmosphere, European Propulsion forum, 1990.
[3] S.M. Correa, Lean premixed combustion for gas turbines: Review and Required research, Fossile Fuel combustion, ASME PD-vol. 33, 1991.
[4] R. Viskanta, Interaction of combustion and heat transfer in porous inert media, in: S.H. Chan (Ed.), Transport Phenomena in Combustion, vol. 1, Taylor & Francis, London, 1995, pp. 64–85.
[5] M. Kaviany, A.A.M. Oliveira, Length scales and innovative use of nonequilibria in combustion in porous media, in: Proceedings of Symposium on Energy Engineering in the 21st century, vol. 1, 2000, pp. 32–56.
[6] S. Zhdanok, L.A. Kennedy, G. Koester, Superadiabatic combustion of methane air mixtures under filtration in a packed bed, Combust. Flame 100 (1995) 221–231.
[7] S.B. Sathe, M.R. Kulkarni, R.E. Peck, T.W. Tong, An experimental and theoretical study of porous radiant burner performance, Twenty-Third Symposium (International) on Combustion/The Combustion Institute 1990, pp. 1011–1015.
[8] L.A. Kennedy, A.A. Fridman, A.V. Saveliev, Superadiabatic combustion in porous media: Wave propagation, instabilities, new type of chemical reactor, Fluid Mech. Res. 22 (1995) 1–26.
[9] G.E. Koester, L.A. Kennedy, V.V. Subramaniam, Low temperature wave enhanced combustion in porous systems, ASME/JSME Thermal Engineering Joint Conference, Hawaii, March 19–24, 1995, pp. 49–55.
[10] K. Hanamura, R. Echigo, S.A. Zhdanok, Superadiabatic combustion in a porous medium, Int. J. Heat Mass Transfer 36 (1993) 3201–3209.

[11] R. Echigo, Effective energy conversion method between gas enthalpy and thermal radiation and application to industrial furnaces, in: Proceedings of the 7th International Heat Transfer Conference, vol. 6, Hemisphere, New York, 1992, pp. 361–366.
[12] F.J. Weinberg, Combustion temperatures: The future? Nature 233 (1971) 239–241.
[13] A. Egerton, K. Gugan, F.J. Weinberg, Combust. Flame 7 (1963) 63–78.
[14] S.B. Sathe, R.E. Peck, T.W. Tong, Flame stabilization and multimode heat transfer in inert porous media: a numerical study, Combust. Sci. Tech. 70 (1990) 93–109.
[15] D.K. Min, H.D. Shin, Laminar premixed flame stabilized inside a honeycomb ceramic, Int. J. Heat Mass Transfer 34 (1991) 341–356.
[16] A.V. Saveliev, L.A. Kennedy, A.A. Fridman, I.K. Puri, Structures of multiple combustion waves formed under filtration of lean hydrogen-air mixtures in a packed bed, Twenty-Sixth Symposium (International) on Combustion/ The Combustion Institute, 1996, pp. 3369–3375.
[17] R. Mital, J.P. Gore, R. Viskanta, A study of the structure of submerged reaction zone in porous ceramic radiant burners, Combust. Flame 111 (1997) 175–184.
[18] P.H. Bouma, L.P.H. De Goey, Premixed combustion on ceramic foam burners, Combust. Flame 119 (1999) 133–143.
[19] I. Glassman, Combustion, third ed., Academic Press, New York, 1996.
[20] M.J. Pilling (Ed.), Low-temperature combustion and autoignition, in: R.G. Compton, G. Hancock (Eds.), Serial book on Comprehensive Chemical Kinetics, vol. 35, Elsevier, Amsterdam, 1997.